Bioorganic Chemistry 64 (2016) 51–58

Contents lists available at ScienceDirect

Bioorganic Chemistry

journal homepage: www.elsevier.com/locate/bioorg

Nitric oxide releasing acridone carboxamide derivatives as reverters of doxorubicin resistance in MCF7/Dx cancer cells

V.V.S. Rajendra Prasad [a,b,*], G. Deepak Reddy [a], Ietje Kathmann [b], M. Amareswararao [c], G.J. Peters [b]

[a] Medicinal Chemistry Research Division, Vishnu Institute of Pharmaceutical Education and Research, Narsapur, India
[b] Department of Medical Oncology, VU University Medical Center, Amsterdam, The Netherlands
[c] Clinical Research Department, Emcure Pharmaceuticals Ltd., Pune, India

ARTICLE INFO

Article history:
Received 15 September 2015
Revised 23 November 2015
Accepted 25 November 2015

Keywords:
Nitric oxide
Acridone
Doxorubicin
Breast cancer

ABSTRACT

A series of nitric oxide donating acridone derivatives are synthesized and evaluated for *in vitro* cytotoxic activity against different sensitive and resistant cancer cell lines MCF7/Wt, MCF7/Mr (BCRP overexpression) and MCF7/Dx (*P*-gp expression). The results showed that NO-donating acridones are potent against both the sensitive and resistant cells. Structure activity relationship indicate that the nitric oxide donating moiety connected through a butyl chain at N^{10} position as well as morpholino moiety linkage through an amide bridge on the acridone ring system at C-2 position are required to exert a good cytotoxic effect. Further, good correlations were observed when cytotoxic properties were compared with *in vitro* nitric oxide release rate, nitric oxide donating group potentiated the cytotoxic effect of the acridone derivatives. Exogenous release of nitric oxide by NO donating acridones enhanced the accumulation of doxorubicin in MCF7/Dx cell lines when it was coadministered with doxorubicin, which inhibited the efflux process of doxorubicin. In summary, a nitric oxide donating group can potentiate the anti-MDR property of acridones.

1. Introduction

Tumor cell resistance to a wide spectrum of anticancer drugs continues to be a major concern for effective cancer chemotherapy. Many different mechanisms have been suggested to explain the development of multidrug resistant (MDR) phenotype in cancer cells, such as alterations in the drug's specific target, reduced uptake or increased efflux of the drug, reduced capacity to enter apoptosis, increase in the ability to repair DNA damage, dissimilar compartmentalization, and an increased rate of detoxification of the drug [1]. One of the mechanisms by which tumors acquire drug resistance is the overexpression of membrane transporters such as drug efflux pump *P*-glycoprotein (*P*-gp/ABCB1) which transports structurally and functionally unrelated compounds. The potential role of *P*-gp in clinical drug resistance stimulated the investigation of various *P*-gp inhibitors in clinical trials [2,3]. Anthracyclines such as doxorubicin, epirubicin and their derivatives are extensively used in the treatment of solid and hematological cancers. However, their efficacy is limited because of their dose dependent cardiotoxicity, an important adverse effect which impairs the patient's outcome and survival [4]. Moreover, resistance to these drugs commonly arises in the cancer cells due to genetic and epigenetic alterations that affect drug sensitivity [1].

It has been demonstrated that HMG-CoA reductase inhibitors such as statins revert doxorubicin resistance in different cancer cell lines [5,6]. Statins, by inhibiting RhoA and its effector Rho kinase, can activate the IKK/NF-kB pathway [7]. By activating NF-kB, statins enhance the transcription of the inducible NO synthase (iNOS) [8], one of the three NOS isoforms, which catalyze the formation of L-citrulline from L-arginine by releasing nitric oxide with a 1:1 stoichiometry [9]. Nitric oxide (NO) is a signaling molecule involved in the control of cellular growth, differentiation and apoptosis [10]. In oxygenated living systems, NO is rapidly converted into nitrite and nitrate [11]. High levels of NO and its metabolic derivatives, the reactive nitrogen species (RNS) can modify functional proteins by *S*-nitrosylation, nitration, disulfide formation leading to bioregulation, inactivation and cytotoxicity particularly in tumor cells [12]. It has been suggested that doxorubicin evokes a significant increase of NO synthesis in murine breast cancer cells and exert its therapeutic effect via an NO-dependent mechanism [13]. Nitric oxide production is quite different in doxorubicin resistant and sensitive cells; restoration of NO production in resistant cells could reverse the MDR in cancer [5]. It was also observed that NO inhibits the efflux of doxorubicin, thus decreasing the resistance of the cell to the drug, further, inducers of NO synthesis such as atorvastatin

* Corresponding author at: Medicinal Chemistry Research Division, Vishnu Institute of Pharmaceutical Education and Research, Narsapur 502313, India.
E-mail address: rajendraprasad.vvs@viper.ac.in (V.V.S. Rajendra Prasad).

http://dx.doi.org/10.1016/j.bioorg.2015.11.007
0045-2068/

and NO donors (GSNO, SNAP and sodium nitroprusside) increased drug accumulation in doxorubicin resistant cells [5]. Further, enhanced histone glutathionylation and reversal of drug resistance was observed after GSNO treatment of MCF7/Dx cells in comparison with MCF7 cells [14].

Nitric oxide plays an important role in numerous physiologic and pathologic processes, including in nonspecific antitumor immune response. New types of NO-releasing hybrid compounds need to be developed to obtain a tissue-specific NO-related function. This creates the possibility that new drugs can be developed which supplement NO exogenously when the body cannot generate sufficient amounts to allow normal biological functions. As a sequel in our research to discover new MDR modulators, we hypothesized that introduction of a NO donating group into a *P*-gp and/or BCRP inhibitor acridone carboxamide moiety would be capable to release NO in a controlled manner and might reverse the doxorubicin resistance in cancer. In the present investigation new set of acridone derivatives are designed based on earlier observations: (i) Acridone-carboxamide analogues are potent inhibitors of the *P*-gp and/or ABCG2 pumps (ii) Controlled NO release in MCF7/Dx cells reverts doxorubicin resistance via enhanced histone glutathionylation (iii) NO donors could affect doxorubicin accumulation through the nitration of tyrosine residues in the drug efflux pumps.

2. Results and discussion

2.1. Chemistry

2.1.1. Synthesis of compounds (1–14)

Nitric oxide releasing acridone derivatives were synthesized according to Scheme 1. Initially acridone-2-carboxylic acid (II) with decent yield (95%) was synthesized by Ullmann condensation reaction of 2-chlorobenzoic acid with *p*-amino benzoic acid to produce 2,4′-iminodibenzoic acid (I), which was then cyclized with polyphosphoric acid instead of sulfuric acid in a water bath at 100 °C for three hours to give acridone-2-carboxylic acid (II). Acridone-2-carboxamides were synthesized by a reaction between an activated form of acridone-2-carboxylic acid (II) and an appropriate amine. A convenient technique for carboxylic group activation was developed that allowed us to synthesize the products in high yields. We prepared an essentially complete set of acridone-2-carboxamides (1–6) whose amide fragments were formed by the alkyl groups or aryl ring systems bearing exocyclic groups at different ring positions.

Further, *N*-alkylation of the different acridone-2-carboxamides (1–6) was achieved by using strong base sodium hydride because the nitrogen atom of the acridone nucleus is normally resistant to undergo *N*-alkylation with alkyl halides due to their weakly basic nature. Compounds (7–10) in good yields obtained by stirring of acridone-2-carboxamides with alkylating agent 1-bromo-3-chloropropane or 1-bromo-4-chloro butane under nitrogen in the presence of potassium iodide at room temperature for 24 h. To introduce the nitric oxide donating moiety, *N*-alkylated acridone-2-carboxamides (7–10) were treated with silver nitrate in dry acetonitrile for three hours. Physical characterization data of all synthesized compounds are shown in Table 1.

All the compounds were separated and purified by column chromatography and/or recrystallization method and dried under high vacuum for more than 12 h. Purified molecules were characterized by using ^{1}H NMR, ^{13}C NMR and Mass spectrometric studies. The ^{1}H NMR spectrum of acridone carboxylic acid (II) showed seven aromatic protons and were resonated at δ7.31–8.52 ppm as multiplet; a singlet at δ11.15 ppm was assigned to N–H proton and one proton of the carboxylic group resonated as singlet at

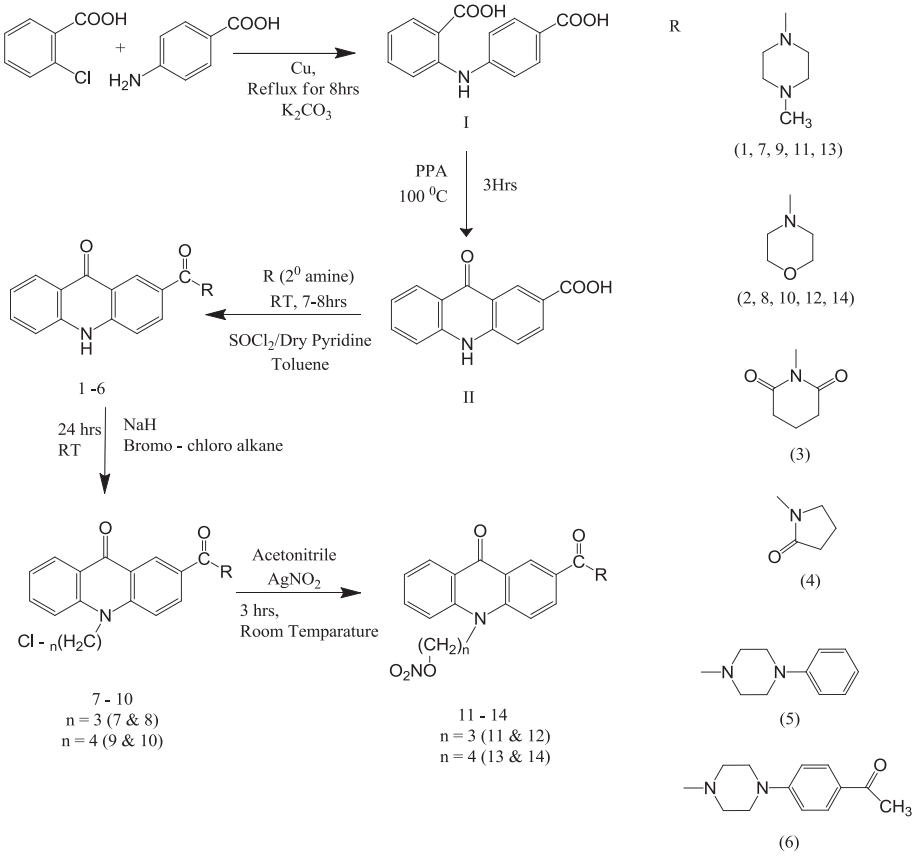

Scheme 1. Synthesis of nitric oxide donating acridone carboxamide derivatives.

δ12.63. Thus, a combination of chemical shift, spin–spin couplings and integration data permitted the identification of individual hydrogen atoms at each side in the aromatic ring. The assignment of protons in all the compounds is fully supported by the integration curves and all the derivatives displayed the characteristic chemical shifts for the acridone nucleus. The ^{13}C NMR spectrum of NO donating acridone carboxamide (11–14) showed 20 signals representing 20 magnetically dissimilar environmental carbons.

Synthesized NO releasing acridone carboxamides were analyzed by mass spectra under ESI conditions. Molecular ions were observed in the form of M + H. The data indicates that as such there is no difference in the fragmentation pattern among the set of acridone series. Overall, mass spectral features of these acridones were similar and straight forward. Most of the compounds yield abundant molecular ions in the form of M + H. All the bonds in the N^{10}-side chain portion are prone to cleavage. This means, that the data presented in this article also demonstrate the usefulness of MS for characterization of acridone derivatives. In conclusion, ^{1}H, ^{13}C NMR and mass spectral data were consistent with the proposed structures.

2.2. Biological

2.2.1. In-vitro cytotoxic activity

The *in vitro* cytotoxic effects of the NO-acridones in comparison with reference drugs doxorubicin (Dx) and mitoxantrone (Mr) were studied by using Sulphorhodamine-B (SRB) assay [15] in the human breast cancer cell line MCF7 and its two drug cross-resistant phenotype sublines (*P*-gp and BCRP), doxorubicin resistant MCF7/Dx (*P*-gp expression) and mitoxantrone resistant MCF7/Mr (BCRP

Table 1
Physical characterization data of nitric oxide donating acridones.

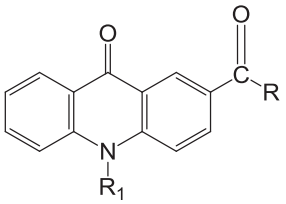

.

Molecule	R1	R	MW	Volume	Log*P*	Yield (%)	M.P (^{0}C)
1	H	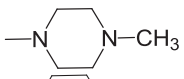	321	885.573	1.81	71	328–330
2	H	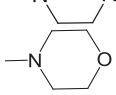	308	824.525	1.65	70	332–334
3	H	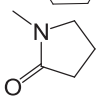	306	956.458	2.73	77	321–325
4	H	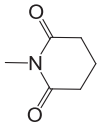	334	1007.481	1.98	74	297–299
5	H	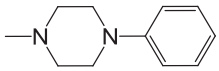	383	1195.715	4.39	73	307–311
6	H	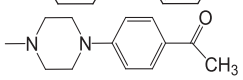	425	1321.636	3.78	70	336–339
7	–$(CH_2)_3$–C1	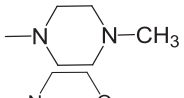	397	1091.580	2.89	76	239–241
8	–$(CH_2)_3$–C1	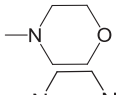	384	1031.632	2.76	68	248–251
9	–$(CH_2)_4$–C1	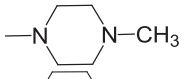	411	1147.389	3.31	66	237–240
10	–$(CH_2)_4$–C1	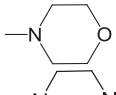	398	1086.715	3.16	71	233–237
11	–$(CH_2)_3$–ONO_2	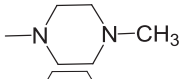	424	1264.463	1.08	62	230–231
12	–$(CH_2)_3$–ONO_2	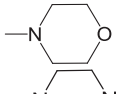	411	1163.379	1.22	69	252–256
13	–$(CH_2)_4$–ONO_2	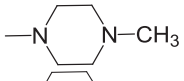	438	1338.013	1.53	69	219–221
14	–$(CH_2)_4$–ONO_2	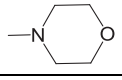	425	1247.593	1.642	71	284–287

Table 2
Cytotoxic activity of acridone carboxamide derivatives against various drug sensitive and resistant cancer cell lines.

Compound	Cell lines/IC_{50} (μM)[a]					
	MCF7/Wt[1]	MCF7/Mr[2]	MCF7/Dx[3]	SW1398[4]	WiDr[5]	LS174T[6]
3	22.0 ± 1.8	32.0 ± 1.4	30.0 ± 1.9	–	–	–
4	30.0 ± 1.5	55.0 ± 1.1	60.0 ± 1.7	–	–	–
5	4.5 ± 0.8	5.1 ± 1.1	6.5 ± 1.2	–	–	–
6	8.5 ± 1.5	10.2 ± 0.9	9.5 ± 0.5	–	–	–
7	18.2 ± 0.9	26.0 ± 1.3	28.2 ± 0.8	–	–	–
8	17.5 ± 0.8	30.1 ± 2.1	26.7 ± 2.0	–	–	–
9	12.6 ± 1.1	22.4 ± 0.6	21.7 ± 1.4	–	–	–
10	10.5 ± 1.6	20.3 ± 1.9	18.5 ± 1.6	–	–	–
11	1.6 ± 0.2	2.1 ± 0.2	3.2 ± 0.4	–	–	–
12	1.2 ± 0.4	1.9 ± 0.1	2.9 ± 0.4	2.9 ± 0.1	4.5 ± 0.8	3.8 ± 1.0
13	1.4 ± 0.6	1.7 ± 0.1	4.2 ± 0.2	11.0 ± 0.7	19.1 ± 1.5	18.2 ± 3.1
14	0.8 ± 0.1	2.7 ± 0.1	1.9 ± 0.1	1.7 ± 0.2	2.8 ± 0.7	3.1 ± 0.3
Mitoxantrone (Mr)	0.090	3.0	–	–	–	–
Doxorubicin (Dx)	0.098	–	3.7	–	–	–

[a] Inhibitory concentrations are presented in Mean ± SEM.
[1] MCF7/Wt: Human breast cancer cell line.
[2] MCF7/Mr: Mitoxantrone resistant MCF7 cells (BCRP overexpression).
[3] MCF7/Dx: Doxorubicin resistant MCF7 cells (*P*-gpexpression).
[4] SW1398: Colorectal cancer cell line.
[5] WiDr: Human colon adenocarcinoma.
[6] LS174T: Human colorectal cancer cell lines.

expression) cell lines. Selected molecules were also screened for their cytotoxic properties against three colorectal cancer cell lines (SW1398, WiDr and LS174T). Each cell line was incubated with eight concentrations (0.5–100 μM) for each compound and was used to create concentration versus growth inhibition curves. The response parameter IC_{50} was calculated for each cell line and tabulated in Table 2.

In the present study, the newly synthesized compounds exhibited an individual potential pattern of selectivity as well as broad-spectrum cytotoxicity against both sensitive and resistant cell lines. Most of the nitric oxide releasing acridones showed activity against the wild type MCF7 cells with IC_{50} values varying from 0.8 μM to 1.6 μM (Table 2). Mitoxantrone resistant MCF7/Mr cells with BCRP expression were sensitive towards the compounds 11, 12, 13 and 14 with IC_{50}values of 1.7–2.7 μM comparable to mitoxantrone (3.0 μM). Regarding doxorubicin resistant MCF7/Dx cells with *P*-gp expression, compounds fused with NO donor, such as compound 11, 12, 13, and 14 exhibited higher cytotoxicity with IC_{50} values of 1.9 μM (compound 14)–4.2 μM (compound 13) comparable to doxorubicin IC_{50} (3.7 μM). Additionally, compounds 12 and 14 also possessed better cytotoxicity against SW1398, WiDr and LS174T cell lines compared to compound 13. However, the cytotoxicity potential of acridone derivatives that were not bearing nitric oxide releasing group was found to be inferior compared to NO donating acridones at lower concentrations against the most of the studied cell lines.

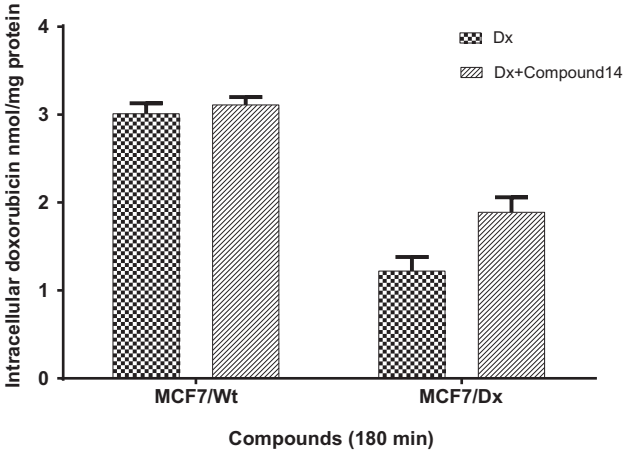

Fig. 1. Intracelular accumulation of doxorubicin in the presence and absence of compound 14 in MCF7 cell lines. To measure the doxorubicin efflux, cell monolayers were treated with 4 μM of doxorubicin with or without nitric oxide donating acridone (compound 14, 50 μM) for 30 min. An extracellular doxorubicin concentration was measured at 180 min by using spectrofluorometer Intragroup statistical calculation are performed using *t*-test and two-tailed *P*-values are reported. Significant increase in the intracellular concentration of doxorubicin is seen in MCF7/Dx cell lines in presence of compound 14 at 180 min ($P = .0076$). No significant difference in intracellular doxorubicin in MCF7/Wt cell lines with or without compound 14 at 180 min ($P = .3125$).

2.2.2. Doxorubicin accumulation and efflux

Earlier studies suggested that doxorubicin sensitive and doxorubicin resistant human colon cancer cells exhibit a different capacity to produce nitric oxide [5] and the doxorubicin resistance is reversed by inducers of NO production, such as cytokines and atorvastatin, or NO releasing compounds. Another study reported implication of NO in the doxorubicin cytotoxicity in HT29 cells and reverts doxorubicin resistance, via the tyrosine nitration of *P*-gp and MRP3, ABC transporters which recognize doxorubicin as a substrate [16]. NO can also inhibit the efflux of doxorubicin (NO donor SNAP), thus decreases the resistance of the cell to the drug. This hypothesis was confirmed by kinetic data [5]. Considering the effect of nitric oxide on the doxorubicin efflux process in *P*-gp expressing cancer cells, in the present study, newly designed nitric oxide releasing acridones were evaluated for their effects on doxorubicin efflux in MCF7/wt and MCF7/Dx (*P*-gp expressing) cell lines. Results of doxorubicin accumulation and efflux in doxorubicin sensitive (MCF7/Wt) and resistant (MCF7/Dx) with and without compound 14 is shown in Figs. 1 and 2 respectively, and the rates of efflux of doxorubicin in combination with and without compound 14 in MCF7/Dx cell lines is shown in Figs. 3 and 4. During 180 min of exposure time, the intracellular levels of doxorubicin significantly increased ($P < .001$). We have also observed a significant reduction ($P = .0004$) in efflux of the doxorubicin into

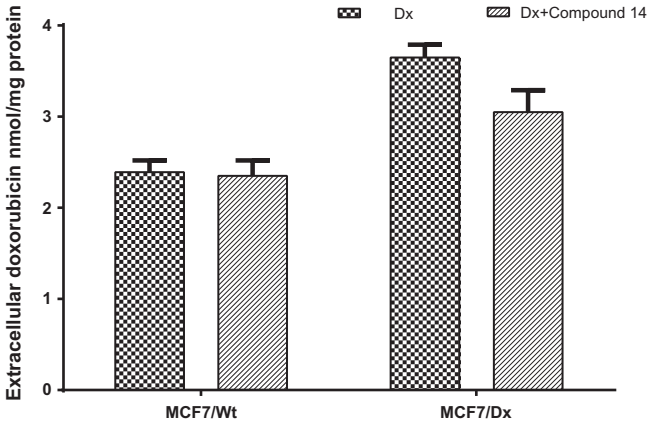

Fig. 2. Efflux of doxorubicin in the presence and absence of compound 14 in MCF7 cell lines. To measure the intracellular doxorubicin concentration, cell monolayers were treated with 4 μM of doxorubicin with or without nitric oxide donating acridone (compound 14, 50 μM) for 30 min. An extracellular doxorubicin concentration was measured at 180 min by using spectrofluorometer. Intragroup statistical calculation are performed using *t*-test and two-tailed *P*-values are reported. No significant difference in doxorubicin efflux concentration in MCF7/Wt cell lines with or without compound 14 at 180 min ($P = .76$). Significant decrease in the efflux concentration of doxorubicin is seen in MCF7/Dx cell lines in presence of compound 14 at 180 min ($P = .021$).

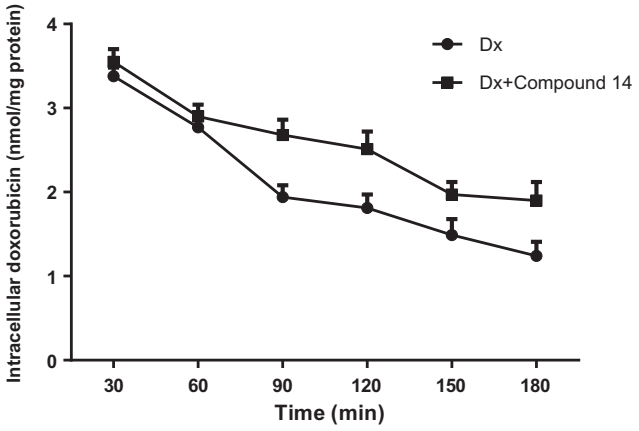

Fig. 3. Time dependent intracellular accumulation of doxorubicin in the presence and absence of compound 14 in MCF7/Dx. To measure the doxorubicin influx, cell monolayers were treated with 4 μM of doxorubicin with or without nitric oxide donating acridone (compound 14, 50 μM) for 30 min. An intracellular doxorubicin concentration was measured at different time intervals (30–180 min). Significant difference in intracellular doxorubicin concentration is seen every time interval in presence of compound 14. Statistical calculations are performed suing *t*-test (two-tailed *P* value at 30 min is .00998, .02 at 60 min, <.001 at 90, 120, 150 and 180 mins).

the extracellular medium in presence of compound 14. When cell lines were treated with doxorubicin along with fixed concentration of nitric oxide releasing acridone for same time intervals, there was no effect observed on doxorubicin accumulation in MCF7/Wt cells ($P = .31$; $P = .76$). However, nitric oxide releasing acridones significantly increased the intracellular concentration of doxorubicin in MCF7/Dx cells ($P = .0076$) by inhibiting the doxorubicin efflux process. In addition, acridone derivatives without nitric oxide donating moiety (1–10) are unable to alter the doxorubicin efflux. These investigations demonstrated that NO donating acridones significantly restored the doxorubicin susceptibility in *P*-gp expressed MCF7/Dx cells by inhibiting the doxorubicin efflux process.

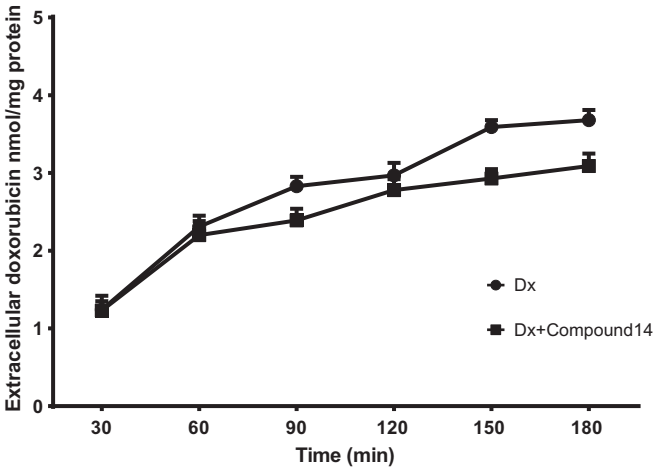

Fig. 4. Time dependent efflux of doxorubicin in the presence and absence of compound 14 in MCF7/Dx. To measure the doxorubicin efflux, cell monolayers were treated with 4 μM of doxorubicin with or without nitric oxide donating acridone (compound 14, 50 μM) for 30 min. An extracellular doxorubicin concentration was measured at different time intervals (30–180 min). Inter-group analysis is performed using ANOVA test. Significant reduction ($P = .0004$) in doxorubicin efflux concentration is seen in presence of compound 14.

Table 3
Exogenous release of nitrite by NO-acridones in MCF7 cancer cells.

Compound	Nitrite concentration was expressed as nano moles of nitrite per 24 h/mg cell protein	
	MCF7/Wt	MCF7/Dx
11	5.21	4.31
12	4.65	3.49
14	7.02	6.64

2.2.3. Nitric oxide release

Exogenous release of nitric oxide by NO-donating acridones might improve the cytotoxicity of acridones as well as affect the role of NO in doxorubicin efflux and influx. Therefore we determined the release of nitric oxide by NO donating acridones by measuring nitrite production in MCF7/Wt and MCF7/Dx (*P*-gp expressing) cell lines. Compounds 11, 12 and 14 were studied for their ability of nitric oxide release (Table 3). Results indicate that nitrite levels in both cell lines were between 3.49 and 7.02 nmol/mg of protein per 24 h. Among the derivatives compound 14 had a higher NO release in MCF7/Wt (7.02 nmol/mg per 24 h) and MCF7/Dx (6.64 nmol/mg per 24 h) cells compared to other investigated molecules. Furthermore, the release of nitric oxide in sensitive and resistant cell line was identical in the experimental condition. Moreover, good associations were observed when cytotoxic data of these molecules compared with exogenous nitrite release.

2.2.4. Molecular docking and binding energy calculations

Molecular docking studies indicated that the TYR 310 and GLN 725 amino acids of *P*-gp protein were associated in binding with newly synthesized molecules (protonated after dissociation of NO group). Ligands such as compound 10 and compound 1 interacted with protein residues GLN 990 and SER 222 respectively. Compound 14 reported highest docking score (−8.610) (Fig. 5). Earlier studies conducted by Dolghih E et al. also reported binding of various *P*-gp inhibitors at the same pocket [17]. Post docking calculation include estimation of ligand binding energy with protein, suggested compound 14 has shown highest binding energy of -83.57 kcal/mol. Protein ligand interactions along with binding energies of acridone derivatives with *P*-gp were shown in Table 4.

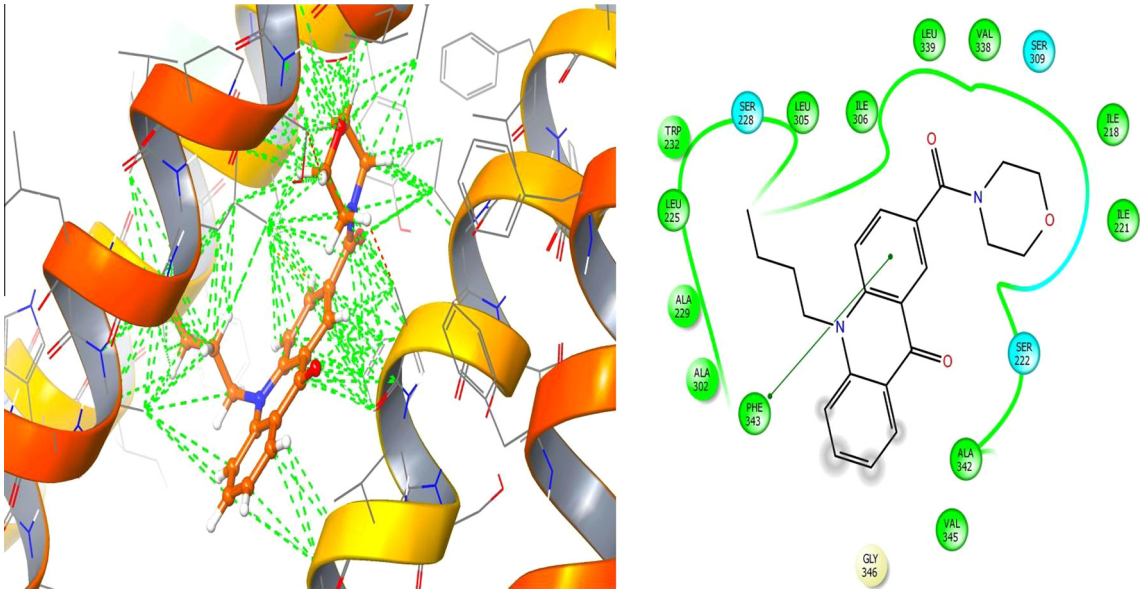

Fig. 5. Interactions of compound 14 with target protein *P*-glycoprotein. Prominent hydrophobic interactions are seen between compound 14 and PHE 343 and other amino acid of docked *P*-glycoprotein.

Table 4
Protein ligand interactions and post docking calculations of novel acridones with *P*-glycoprotein.

Compound	Dock score	No of H-bonds	Interacting amino acids	H-bond distance (Å)	Binding energy
14	−8.610	0	–	–	−83.571604
13	−7.411	1	GLN 725	1.83	−76.915953
5	−6.825	0	–	–	−70.954276
10	−6.718	1	GLN 990	1.91	−68.425796
3	−6.274	0	–	–	−67.854175
6	−6.196	0	–	–	−62.197424
4	−6.097	0	–	–	−66.741288
9	−6.178	1	TYR 310	2.23	−60.745826
12	−5.93	0	–	–	−59.271147
2	−5.739	0	–	–	−55.412975
7	−5.618	1	TYR 310	2.08	−56.124834
11	−5.482	2	TYR 310 GLN 725	2.36 2.71	−53.943285
8	−5.198	0	–	–	−59.215846
1	−5.014	1	SER 222	1.84	−54.158622

3. Conclusions

Several newly developed nitric oxide donating acridone carboxamides were active in drug sensitive and resistant cell lines and could reverse MDR, which might be related the nitric oxide release rate. We used the fluorescent nature of doxorubicin to determine the altered abilities of MCF7/Wt and MCF7/Dx (*P*-gp expressed) cells to accumulate doxorubicin during 180 min of exposure in the presence and absence of nitric oxide releasing acridone. The results from the cytotoxicity assays, *in vitro* nitrite release, and drug accumulation studies clearly indicate that NO donating acridones had a remarkable rate of nitrite release and cytotoxic effects. Moreover, the present studies also demonstrated that exogenous release of nitric oxide by NO donating acridones enhanced the accumulation of doxorubicin in MCF7/Dx cell lines when it is coadministered with doxorubicin by inhibiting efflux process. It is also clear that presence of NO group potentiated the cytotoxic effect of the acridone derivatives. Further, nitric oxide donating group could potentiate the N^{10}-substituted acridones to reverse the doxorubicin resistance in MCF7/Dx cells.

4. Experimental

4.1. Materials and methods

All chemicals and solvents were supplied by Sigma Aldrich, S.D. Fine Chemicals Ltd, Bangalore India. Reactions were monitored by thin layer chromatography (TLC) and compounds were purified by using column chromatography with silica gel Merck Grade 60 (230–400 mesh, Merck, Germany). Melting points were recorded on a Tempirol hot-stage with microscope (AGA International, India) and were uncorrected. Nitric oxide releasing acridone derivatives were characterized by ^{1}H and ^{13}C NMR in DMSO-d_6 solution in a 5 mm tube on a Brukerdrx 500 Fourier transform spectrometer (Bruker Bioscience, USA) and tetra methyl silane (TMS) was used as an internal standard. Chemical shifts were expressed as δ (ppm) values. The spectrometer was internally locked to deuterium frequency of the solvent. Acridones were also characterized by ESI-MS spectrometry. Collision-induced dissociation (CID) spectra were acquired in the positive ion mode on an MDS Sciex (Concord, Ont., Canada) API 4000 triple quadrupole mass spectrometry with direct infusion of each acridone at a concentration of 10 μM in 50% methanol, at flow rate of 25 μL/min. The instrument was operated with a spray voltage of 5.5 kV, a declustering potential of 50 eV, a source temperature of 100 °C, a GSI value of 50 and the curtain gas set at 10. Ultra-pure nitrogen was used as both curtain gas and collision gas. MS/MS spectra of the protonated molecule of each drug were acquired and multiple reaction monitoring (MRM) transition for important fragments were monitored as the collision energy was ramped from 5 V to 100 V (step size 0.5 V). The data for the fragment-ion curves represent an average of five consecutive experiments. The nitrate/nitrite release rates from individual derivatives in the cells were determined by a colorimetric assay using the nitrate/nitrite colorimetric assay kit (Sigma Aldrich, The Netherland), according to the manufacturer's instructions.

4.2. In-vitro cytotoxic studies by SRB assay

The nitric oxide releasing acridone derivatives were evaluated for their cytotoxic activity against different cancer cells

(MCF7/Wt, MCF7/Dx, MCF7/Mr, SW1398, WiDr, LS174T) by using the sulforhodamine B (SRB) assay [15]. In brief, cells were cultured in RPMI 1640 supplemented with 10% fetal calf serum, and cultures were passaged once or twice a week using trypsin EDTA to detach the cells from their culture flasks. The fast-growing cells were harvested, counted and plated at suitable concentrations in 96-well microplates. Cells were allowed to adhere for 24 h. Thereafter one plate was fixed to determine the initial absorbance (T_0). To the other plates compounds dissolved in the culture medium were added to the culture wells in triplicate and incubated further for 72 h at 37 °C under 5% CO_2 atmosphere. The cultures were fixed with cold TCA and stained with0.4% SRB dissolved in 1% acetic acid. After dissolving the bound stain with 150 μL of 10 mM unbuffered Tris base (Tris(hydroxymethyl)aminomethane) solution using gyratory shaker, absorbance was measured at 540 nm using a microplate reader (Tecan). Growth was calculated by correcting the control plate (without drugs) cultured for 72 h (T_{72} control) with the T_0 plate. Growth inhibition was calculated as: $(T_{72}$ drug $- T_0)/(T_{72}$ control $- T_0) * 100\%$. The efficacy of the compounds was compared by estimating the concentration required to inhibit cellular growth by 50% (i.e., IC_{50}) from each separate growth inhibition curve. Each value represents the mean of triplicate experiments.

4.3. Doxorubicin accumulation and efflux studies by spectrofluorometer

Doxorubicin sensitive and resistant MCF7 cells (7×10^5/well) were grown in 35 mm diameter Petri dishes. Before every test, cells were washed and cultured in fresh medium without doxorubicin for 24 h. Later, cells were incubated in 2 ml medium containing 4 μmol/L doxorubicin with or without nitric oxide donating acridones (50 μM) for different time intervals (30–180 min), washed twice in ice-cold PBS and harvested using trypsin/EDTA (0.05/0.02% v/v). Cells were centrifuged for 3 min at 15,000 rpm (4 °C) and re-suspended in 1 mL of a 1:1 mixture of ethanol/0.3 N HCl. Then 50 μL of the cell suspension was used for measurement of cellular proteins. The remaining part was checked for the doxorubicin content using a Fluor-max spectrofluorimeter. Excitation and emission wavelengths were 475 nm and 553 nm, respectively. A blank was prepared in the absence of cells in every set of experiments and its fluorescence was subtracted from that obtained in the presence of cells. Fluorescence was converted in nanomoles of doxorubicin per milligram of cellular protein, using a calibration curve prepared previously. To measure the drug efflux, cell monolayers were incubated with 4 μmol/L doxorubicin for 30 min; cells were washed twice with PBS and incubated in fresh 5 ml of PBS, then 0.5 mL of supernatant was taken at different time intervals (15–180 min) and checked for doxorubicin associated fluorescence as described above.

4.4. Nitrite measurement in vitro

The levels of nitrite formed from individual compounds in the cells were determined by a colorimetric assay using the nitrate/nitrite colorimetric assay kit (Sigma Aldrich, The Netherland), according to the manufacturer's instructions. Confluent cell monolayers (6×10^5/well) in 35 mm diameter Petri dishes were treated in triplicate with 25 μM NO releasing acridone and incubated for 24 h under the experimental conditions. The cells were washed twice in ice-cold PBS and harvested using trypsin/EDTA (0.05/0.02% v/v). Cells were centrifuged for 5 min at 15,000 rpm (4 °C) and re-suspended in 1 mL of a 1:1 mixture of ethanol/0.3 N HCl. Nitrite production was measured by mixing 100 μL of cell lysates with 100 μL of Griess reagent in a 96 well plate and after 30–300 min incubation at 37 °C in the dark, absorbance was measured at 540 nm with a Tecan microplate reader. Then50 μL of the cell suspension was used for measurement of cellular proteins. A blank was prepared for each experimental condition in the absence of cells, and its absorbance was subtracted from that obtained in the presence of cells. Nitrite concentration was expressed as nanomoles of nitrite per 24 h/mg of cellular protein.

4.5. Molecular docking and binding energy calculations

In silico binding interactions of *P*-gp & newly synthesized acridones was performed by using Glide XP algorithm of Schrodinger Suite. Digital crystal structure of *P*-gp protein was retrieved from the PDB website (PDB ID: 4Q9H) and was processed by removing non protein components and adding missing amino acids and hydrogen atoms to satisfy the valence and optimized by using OPLS-2005 force field. Binding pockets were identified and a receptor grid was generated and ligands (energy minimized) were docked [18]. The terminal NO group of each compound is replaced with protonation in order to understand the binding pattern of the acridone which is protonated after dissociation of NO donor group. Later, to the docked complexes MM/GBSA calculations were performed to determine the binding energy [18]. The total free energy of binding is then expressed in the form below mentioned equation:

$\Delta G_{bind} = G_{complex} - (G_{protein} + G_{ligand})$ where ΔG_{bind} is ligand binding energy

In other terms,

$$\Delta G_{bind} = \Delta E_{gas} + \Delta G_{solvation} - T\Delta S$$

where gas phase molecular mechanical energy is ΔE_{gas} (i.e. Contributions from the van der Waals energy, electrostatic energy, and internal energy), the solvation free energy are $\Delta G_{solvation}$ (polar and non-polar contributions) and $T\Delta S$ is the entropy [19].

4.6. Synthesis and chemical characterization

4.6.1. Preparation of 2,4′-iminodibenzoic acid (I): Ullmann Condensation

To a mixture of *o*-chloro benzoic acid (7.8 g, 0.05 mol), *p*-amino benzoicacid (6.85 g, 0.05 mol) and copper powder (0.2 g) in 60 mL isoamyl alcohol, dry potassium carbonate (5 g) was slowly added and the contents were allowed to reflux for 6–8 h on an oil bath at 160 °C. The isoamyl alcohol was removed by steam distillation and the mixture was poured into one liter of hot water and acidified with concentrated hydrochloric acid. Precipitate was filtered, washed with hot water and collected. The crude acid was dissolved in aqueous sodium hydroxide solution, boiled in the presence of activated charcoal and filtered. On acidification of the filtrate with concentrated hydrochloric acid, a light yellowish precipitate was obtained which was washed with hot water and recrystallized from aqueous methanol to give light yellow solid (yield 91%, mp 187 °C).

4.6.2. Synthesis of acridone-2-carboxylic acid (II)

Five grams of 2,4′-iminodibenzoic acid (I) was put into a round bottom flask and 50 grams of polyphosphoric acid was added. The reaction mixture was shaken well and heated on a water bath at 100 °C for 3 h. Appearance of yellow color indicated the completion of the reaction. Then, it was poured into one liter of hot water and made alkaline by liquor ammonia. The yellow precipitate was filtered and collected. The acridone-2-carboxylic acid (II) was recrystallized from acetic acid (yield 89%, mp 326–328 °C). Further, purity of the compound was checked by TLC and the purified product was characterized by spectral methods.

^{1}H NMR (DMSO-d_6) δ ppm: 12.63 (s, 1H, OH), 11.15 (s, 1H, NH), 7.31–8.52 (m, 7H, Ar–H). **^{13}C NMR (DMSO-d_6) δ ppm**: 172.4, 169.4,

156.2, 143.5, 140.4, 137.4, 134.3, 132.4, 131.2, 128.3, 126.3, 125.5, 122.4. **ESI-MS (m/z, %)**: 239.21 (100).

4.6.3. General method of preparation of acridone carboxamides (1–6)

To the suspension of compound II (1 gm, 4.18 mmol) in 15 ml of dry toluene, thionyl chloride (0.42 ml, 5.81 mmol) and freshly dried pyridine (0.46 ml, 5.81 mmol) were added. The reaction mixture was stirred at room temperature for 3–4 h and then combined with excess of secondary amines and triethylamine (1.72 ml, 12.37 mmol) and stirred for another 3 h. The reaction was monitored by TLC. The following day the solvent was removed under vacuum and water was added to the solid residue. The precipitate was filtered, washed with water and dried. The crude product was crystallized from n-butanol-DMF (19:1).

1: ^{1}H NMR (DMSO-d_6) δ ppm: 10.85 (s, 1H, NH), 7.38–8.57 (m, 7H, Ar–H), 2.94 (t, 8H, CH_2–N–CH_2–CH_2–N–CH_2), 2.98 (s, 3H, N–CH_3). **^{13}C NMR (DMSO-d_6) δ ppm**: 173.1, 168.2, 159.5, 141.4, 140.5, 136.1, 135.7, 134.7, 130.8, 127.2, 126.4, 124.7, 123.6, 56.8. 54.3, 47.8, 46.3.**ESI-MS (m/z,%):** 321.7 (80).

4.6.4. N-alkylation of acridone carboxamide (7–10)

Substituted acridone-carboxamide (310 mg, 1 mM) was dissolved in 25 ml of dry DMF and then added NaH (120 mg). Then the reaction mixture was stirred under nitrogen at room temperature for 60 min and 1-bromo-3-chloropropane or 1-bromo-4-chloro butane (2 mM), potassium iodide (150 mg) added slowly into the reaction mixture and stirred for 24 h at room temperature. Water was slowly added under ice bath with rapid stirring. The crude yellow color product was collected and purified.

7: ^{1}H NMR (DMSO-d_6) δ ppm: 7.41–8.53 (m, 7H, Ar–H), 2.71–2.82 (t, 8H, CH_2–N–CH_2–CH_2–N–CH_2),2.91 (t, 2H, N–$\underline{CH_2}$–CH_2–CH_2–Cl), 3.43 (t, 2H, N–CH_2–CH_2–$\underline{CH_2}$-Cl), 2.12 (m, 2H, N–CH_2–$\underline{CH_2}$–CH_2–Cl), 3.14 (s, 3H, N–CH_3) **^{13}C NMR (DMSO-d_6) δ ppm**: 172.5,164.9, 156.3, 141.6, 140.1,137.3, 136.2, 135.2, 133.1, 129.1, 128.6, 126.2, 124.5, 61.2, 59.2, 58.6. 56.3, 55.9, 49.4, 46.4, 34.2. **ESI-MS (m/z,%):** 398.9 (55).

4.6.5. Nitration of N-alkylated acridone carboxamide (11–14)

A solution of the appropriate haloalkyl derivative in dry acetonitrile (2 ml) was treated portion wise with a solution of $AgNO_3$ (0.34 g, 2 mmol) in dry acetonitrile (5 ml) and the whole mixture was stirred at room temperature for 3 h; the reaction was monitored by TLC. The mixture was then filtered, evaporated to dryness then residue was recrystallized.

11: ^{1}H NMR (DMSO-d_6) δ ppm: 7.48–8.51 (m, 7H, Ar–H), 2.68–2.91 (t, 8H, CH_2–N–CH_2–CH_2–N–CH_2), 3.12 (t, 2H, N–$\underline{CH_2}$–CH_2–CH_2–ONO_2), 4.42 (t, 2H, N–CH_2–CH_2–$\underline{CH_2}$–ONO_2), 2.02 (m, 2H, N–CH_2–$\underline{CH_2}$–CH_2–ONO_2), 3.12 (s, 3H, N–CH_3). **^{13}C NMR (DMSO-d_6) δ ppm:** 172.4, 161.6, 157.6, 144.6, 143.2, 137.1, 136.3, 135.3, 132.5, 128.4, 127.4, 126.3, 124.3, 68.6, 59.6, 58.2, 55.5, 53.3, 48.7, 47.8, 37.3. **ESI-MS (m/z,%):** 425.6 (68).

12: ^{1}H NMR (DMSO-d_6) δ ppm: 7.51–8.59 (m, 7H, Ar–H), 2.81 (t, 4H, CH_2–N–CH_2), 2.92 (t, 4H, CH_2–O–CH_2), 3.03 (t, 2H, N–$\underline{CH_2}$–CH_2–CH_2–ONO_2), 4.63 (t, 2H, N–CH_2–CH_2–$\underline{CH_2}$–ONO_2), 2.15 (m, 2H, N–CH_2–$\underline{CH_2}$–CH_2–ONO_2). **^{13}C NMR (DMSO-d_6) δ ppm:** 171.6, 162.4, 158.1, 143.7, 141.5, 139.4, 136.6, 135.1, 133.4, 129.7, 128.1, 126.4, 124.9, 68.4, 59.5, 58.3, 55.2, 54.2, 49.5, 48.2. **ESI-MS (m/z,%):** 412.8 (40).

14: ^{1}H NMR (DMSO-d_6) δ ppm: 7.32–8.45 (m, 7H, Ar–H), 2.65 (t, 4H, CH_2–N–CH_2), 2.89 (t, 4H, CH_2–O–CH_2), 3.16 (t, 2H, N–$\underline{CH_2}$–CH_2–CH_2–CH_2–ONO_2), 4.58 (t, 2H, N–CH_2–CH_2–CH_2–$\underline{CH_2}$–ONO_2), 2.27 (m, 4H, N–CH_2–$\underline{CH_2}$–$\underline{CH_2}$–CH_2–ONO_2). **^{13}C NMR (DMSO-d_6) δ ppm:** 172.1, 163.5, 158.4, 143.3, 142.4, 139.5, 136.2, 134.4, 133.6, 128.4, 127.1, 126.6, 125.3, 65.5, 59.4, 58.4, 57.9, 55.3, 54.1, 50.5, 49.3. **ESI-MS (m/z,%):** 426.7 (50).

Acknowledgments

Dr. V.V.S. Rajendra Prasad would like to acknowledge the funding support from SERB, Department of Science and Technology (DST), Government of India under "Fast Track Scheme" [SR/FT/LS-175/2009] and Laboratory Medical Oncology, VU University Medical Center (VUMC), Amsterdam, The Netherlands for providing necessary research facilities to carry out the cytotoxicity studies.

References

[1] M.M. Gottesman, T. Fojo, S.E. Bates, Nat. Rev. Cancer 2 (2002) 48–58.
[2] P. von Bossanyi, S. Diete, K. Dietzmann, M.W. Kirches, E. Kirches, Acta Neuropathol. 94 (1997) 605–611.
[3] H. Thomas, H.M. Coley, Cancer Causes Control 10 (2003) 159–165.
[4] G. Bonadonna, S. Monfardini, Lancet 1 (1969) 837.
[5] C. Riganti, E. Miraglia, D. Viarisio, C. Costamagna, G. Pescarmona, D. Ghigo, A. Bosia, Cancer Res. 65 (2005) 516–525.
[6] C. Riganti, S. Orecchia, G. Pescarmona, P.G. Betta, D. Ghigo, A. Bosia, Int. J. Cancer 119 (2006) 17–27.
[7] R.S. Rattan, A.K. Giri, I. Singh, Free Radic. Biol. Med. 35 (2003) 1037–1050.
[8] F.R. Greten, M. Karin, Cancer Lett. 206 (2004) 193–199.
[9] C. Nathan, Q.-W. Xie, J. Biol. Chem. 269 (1994) 13725–13728.
[10] G. Magrinat, S.N. Mason, P.J. Shami, J.B. Weinberg, Blood 80 (1992) 1880–1884.
[11] D.A. Wink, J.B. Mitchell, Free Radic. Biol. Med. 25 (1998) 434–456.
[12] J.M. Fukuto, D.A. Wink, Met. Ions Biol. Syst. 36 (1999) 547–554.
[13] D.S. Lind, M.I. Kontaridis, P.D. Edwards, M.D. Josephs, L.L. Moldawer, E.M. Copeland, J. Surg. Res. 69 (1997) 283–287.
[14] A. de luca, N. Moroni, Annaluciaserafino, A. Primavera, A. Pastore, J. Pedersen, R. Petruzzelli, M. Graziafarrace, P. Pierimarchi, G. Moroni, G. Federici, P. Sinibaldi Vallebona, M. Bello, Bio. Chem. J. 440 (2011) 175–183.
[15] Y.P. Keepers, P.E. Pizao, G.J. Peters, et al., Eur. J. Cancer 27 (1991) 897–900.
[16] S. Doublier, C. Riganti, C. Voena, C. Costamagna, E. Aldieri, G. Pescarmona, D. Ghigo, A. Bosia, Mol. Cancer Res. 6 (2008) 1607–1620.
[17] E. Dolghih, C. Bryant, A.R. Renslo, M.P. Jacobson, PLoS Comput. Biol. 7 (2011) e1002083.
[18] V.V. Rajendra Prasad, G. Deepak Reddy, D. Appaji, G.J. Peters, Y.C. Mayur, J. Mol. Graph. Model. 40 (2013) 116–124.
[19] C. Muñoz, F. Adasme, J.H. Alzate-Morales, J. Mol. Graph. Model. 32 (2012) 39–48.